


## Article

# Beak Microstructure Estimates of the Age, Growth, and Population Structure of Purpleback Flying Squid (*Sthenoteuthis oualaniensis*) in the Xisha Islands Waters of the South China Sea

Ziyue Chen <sup>1</sup>, Huajie Lu <sup>1,\*</sup> , Wei Liu <sup>2</sup>, Kai Liu <sup>1</sup> and Xinjun Chen <sup>1,3,4,5,6</sup><sup>1</sup> College of Marine Sciences, Shanghai Ocean University Shanghai, Shanghai 201306, China;

d200200053@st.shou.edu.cn (Z.C.); m190200611@st.shou.edu.cn (K.L.); xjchen@shou.edu.cn (X.C.)

<sup>2</sup> Hainan Academy of Ocean and Fisheries Science, Haikou 570100, China; wliu0723@163.com<sup>3</sup> The Key Laboratory of Sustainable Exploitation of Oceanic Fisheries Resources, Shanghai Ocean University, Ministry of Education, Shanghai 201306, China<sup>4</sup> National Distant-Water Fisheries Engineering Research Center, Shanghai Ocean University, Shanghai 201306, China<sup>5</sup> Key Laboratory of Oceanic Fisheries Exploration, Ministry of Agriculture, Shanghai 201306, China<sup>6</sup> Scientific Observing and Experimental Station of Oceanic Fishery Resources, Ministry of Agriculture and Rural Affairs, Shanghai 201306, China

\* Correspondence: hjlu@shou.edu.cn; Tel.: +86-021-6190-0318



**Citation:** Chen, Z.; Lu, H.; Liu, W.; Liu, K.; Chen, X. Beak Microstructure Estimates of the Age, Growth, and Population Structure of Purpleback Flying Squid (*Sthenoteuthis oualaniensis*) in the Xisha Islands Waters of the South China Sea. *Fishes* **2022**, *7*, 187. <https://doi.org/10.3390/fishes7040187>

Academic Editor: Gioele Capillo

Received: 5 July 2022

Accepted: 23 July 2022

Published: 26 July 2022

**Publisher's Note:** MDPI stays neutral with regard to jurisdictional claims in published maps and institutional affiliations.



**Copyright:** © 2022 by the authors. Licensee MDPI, Basel, Switzerland. This article is an open access article distributed under the terms and conditions of the Creative Commons Attribution (CC BY) license (<https://creativecommons.org/licenses/by/4.0/>).

**Abstract:** This study aimed to explore the feasibility of using an upper beak microstructure to estimate the age of purpleback flying squid (*Sthenoteuthis oualaniensis*). From these microstructures, the age and growth of squid caught from January to March and May to August in 2018, 2019, and 2020 in the waters surrounding the Xisha Islands in the South China Sea were determined. We found three typical growth zones (the hood region, crest region, and axis), abnormal increments (checks), and erosion in the beak examination. The average dorsal mantle length (ML) of males and females was 112.13 ( $\pm 15.23$  mm) and 119.67 mm ( $\pm 24.50$  mm), respectively, and no squid were older than 10 months. The peak hatching dates, according to back calculations, were from October to January of the next year. All sampled squid belonged to the autumn/winter cohort. Significant sex differences were found in the relationship between ML and age in squid with similar growth patterns. Exponential models best described the relationships of ML with age and body weight (BW) for both sexes. However, a linear model best described the relationship between age and upper rostrum length (URL). The maximum absolute daily growth rates (AGR) of BW were reached during days 240–270 for both sexes. The maximum AGRs in ML were reached during days 180–210 and 240–270 for males and females, respectively. The period of 120–150 days (4–5 months) was considered the sub-adult stage of *S. oualaniensis* in the Xisha Islands waters of the South China Sea. This study confirmed that the beak microstructure provides good age estimates for purpleback flying squid (*S. oualaniensis*).

**Keywords:** *Sthenoteuthis oualaniensis*; beak; age; growth pattern; South China Sea

## 1. Introduction

The purpleback flying squid, *Sthenoteuthis oualaniensis*, is one of the most abundant commercial resources of oceanic cephalopods and predominantly inhabits warmer waters in the subequatorial and equatorial Indo-Pacific Ocean [1]. The northwestern Indian Ocean and Arabian Sea are thought to be high-density areas for this important oceanic resource, as determined by a preliminary investigation conducted by the former Union of Soviet Socialist Republics (USSR) from the 1960s to the 1980s [2,3]; initially, commercial investigation and exploitation were undertaken by Chinese squid jigging vessels from 2003 to 2005 [4]. The total biomass of *S. oualaniensis* is estimated to be 5–7 million tons in the subtropical and

tropical Pacific Ocean, and it is usually randomly caught as bycatch [1]. Despite its wide geographic distribution in the western Pacific Ocean, this resource has been inadequately exploited; in the past 40 years, it has been caught only in waters around China's Taiwan Province and Okinawa, including by small-scale commercial jigging fisheries and local artisanal fisheries [1,5]. However, a recent survey detected more than 1 million tons of total *S. oualaniensis* biomass through an acoustic survey in the South China Sea, demonstrating considerable potential to sustain relatively ample yields [6]. In the South China Sea, *S. oualaniensis* have been mostly caught and stored as bycatch by Chinese fishing vessels equipped with light traps and falling nets in recent years, a relatively inadequate exploitation and utilization of this abundant resource [7,8].

Previous studies have generally established the fishery biology characteristics of *S. oualaniensis* in different areas, including its population structure, age and growth, diet and behavior, reproduction, and ecology. Because of its complex population structure and wide geographic distribution, several different intraspecific forms have been divided on the basis of distinct differences in mature body size, dorsal photophores, and life span [1,9]. *S. oualaniensis* is an active predator with a wide feeding spectrum in marine ecosystems; it feeds on small fishes and crustaceans and even demonstrates considerable cannibalism [1,4,10,11]. Along with its high daily dietary intake, *S. oualaniensis* exhibits a rapid growth rate over its short life span [1,11,12]. Moreover, *S. oualaniensis* is frequently found in the diet of predatory fishes, marine mammals, and birds [1,11,12]. As this species serves as both prey and predator, it may link trophic levels in the marine ecosystem [13–15].

In cephalopods, the beak is the feeding organ and is embedded in the muscle of the buccal mass [16]. Because of its composition (consisting of protein and chitin fibers), the beak is one of the few hard structures in cephalopods and is characterized by resistance to erosion, a stable shape, and a stiff structure [16,17]. Studies of the fishery biology and ecology of cephalopods found that the beak can help to determine taxonomy, age and growth patterns, and pigmentation, as well as to estimate biomass [18–21]. Previous growth studies have summarized the morphological characteristics and growth patterns of *S. oualaniensis* statoliths [22–27], but fewer studies have explored the growth pattern and pigmentation of *S. oualaniensis* beaks [28–32].

It is difficult to feed these short-lived oceanic squids under artificially experimental conditions [33]. This particular issue increased the difficulty for us to deeply understand the details of their growth pattern and whole life history. It is necessary to explore the age and growth information for sufficient development of this fishery resource. Estimating age and growth patterns could provide valuable information and a basis for fishery biology, ecology, and resource management. This age and growth information could apply for fishery biology, ecology, and stock assessment management, which includes size-at-age, maturity, and life-history parameters [34]. Environmental information was also closely related to the age and growth pattern, and it clearly reflected in the growth rate of squids in time-specific stage [34]. Differences of age structures and growth patterns were easily found between different populations and life stages, especially in *S. oualaniensis* [1]. Because of different body length forms and their complicated population structures of squids, estimating the age structures and growth patterns of squids with the length-frequency method is inaccurate [34]. However, clear daily growth increments are obvious in sections of squid statoliths, eye lenses, and beaks [35–37]. In general, previous age and growth studies mostly analyzed the statoliths of cephalopods, but studies on cephalopod beaks are relatively scarce. Early studies on the age and growth pattern of squids mainly analyzed periodically deposited increments in the statolith microstructure [38]. In recent years, the number of growth studies has increased, paralleling the gradual increase in the exploitation of important commercial species, especially ommastrephid and loliginid squids [34,35,39]. Many previous studies have examined the age and growth pattern of statolith microstructures among many species of squids in the last several decades, including *Dosidicus gigas*, *Ommastrephes bartramii*, and *Sthenoteuthis pteropus* [35,40–42]. These

studies have suggested that age and growth patterns provide valuable information on the life history of cephalopods.

Compared with tiny statoliths, it is much easier to extract beaks from squid heads without destroying them. Additionally, beak specimens may be more conveniently preserved in the long term [33,43]. To decrease the high failure rate caused by the tiny size of the statolith, identification of a substitute aging tool is needed [44]. In squid beaks, a daily concentric increment in the lateral wall surface (LWS) can be clearly observed and is thought to represent 1 day in the larval stage [36]. Age estimations according to daily increments in the LWS of the beak are more convenient than those of statoliths [45]. Additionally, many clear periodic longitudinal light and dark bands have been found in the rostrum sagittal section (RSS) of beaks [46]. The RSS is usually used to estimate age because age estimation from this section is more accurate than that of the LWS [45]. Records of environmental events and life history information are obviously reflected by stress marks [47]. The upper beak is more suitable for age estimations than the lower beak because the lower beak usually exhibits erosion during the feeding period [48]. The erosion of RSS is often caused by feeding behavior; however, the dorsal region of the hood may be used instead to eliminate bias in the estimation [45]. Examination of octopus beak microstructure revealed that each daily increment in the RSS corresponds to one day in life history [49]. The daily RSS increments have also been applied in growth studies of *D. gigas* and *O. bartramii*; in these species, the number of beak increments was closely related to the number of statolith increments [39,43,48]. Therefore, the upper beak is considered a tool for estimating the age and describing the growth pattern of cephalopods [20].

In our study, we explored the age and growth pattern of *S. oualaniensis* found in the waters surrounding the Xisha Islands in the South China Sea with examinations of the upper beak microstructure. This study is the first to use beak microstructure as a tool based on age back-calculation to estimate age, identify hatching groups, and analyze the growth pattern of *S. oualaniensis*. Growth patterns were evaluated according to the relationships between mantle length (ML) and body weight (BW), as well as between age and ML and BW growth rates. To establish a basis for this species' fishery biology, ecology, and life history, it is essential to obtain an in-depth understanding of its age and growth pattern in the South China Sea. This study will provide valuable information for age estimation research and the efficient exploitation of *S. oualaniensis*, which is an important squid resource in the South China Sea.

## 2. Materials and Methods

### 2.1. Squid Sampling

A total of 1460 squid samples were randomly caught and collected in the survey by the Chinese fishing vessels Qiong Sanya 72106 and Qiong Sanya 72060 (equipped with light traps and falling nets) in the waters surrounding the Xisha Islands in the South China Sea (12°18' N–18°46' N, 110°10' E–115°58' E) from January to March and May to August in 2018, 2019, and 2020 (Figure 1). All squid samples were immediately frozen on the ship and dissected in the laboratory.

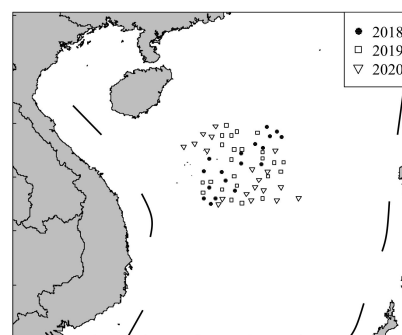


**Figure 1.** Site of investigations and samples for *S. oualaniensis*.

## 2.2. Fishery Biology Measurements

Fishery biology data were observed and measured after squid were thawed in the laboratory; mantle length (ML) and body weight (BW) were measured to the nearest 1 mm and 1 g, respectively. Samples were categorized in terms of sex according to the morphological characteristics of the gonads previously established, and 5 age stages were identified (immature: I and II; maturing: III; mature: IV and V) [30,43,50]. The upper and lower beaks were removed from the buccal mass of the head, cleaned, and then preserved with 75% alcohol solution. The following 12 morphological variables, namely, upper hood length (UHL), upper crest length (UCL), upper rostrum length (URL), upper rostrum width (URW), upper lateral wall length (ULWL), upper wing length (UWL), lower hood length (LHL), lower crest length (LCL), lower rostrum length (LRL), lower rostrum width (LRW), lower lateral wall length (LLWL), and lower wing length (LWL), were measured to the nearest 0.1 mm by a Vernier caliper [30,48].

## 2.3. Beak Processing and Aging

We selected upper beaks from the samples to avoid bias during age estimation as much as possible because lower beaks are more frequently eroded during feeding behavior [48]. All age increments appear on the focal plane of the hood of the beak. We selected the rostrum sagittal section (RSS) instead of the lateral wall surface (LWS) for precise estimation [45]. After cleaning the upper beak with water, the RSS was cut into two unequal pieces by a cutter bar; the larger piece was immobilized and gradually hardened in a plastic mold with cakey epoxy [48]. The focal plane sample was sanded with different types of coarse sandpapers (grit: 120, 600, 1200, and 2000) and polished with smooth sandpaper (2400) with aluminum oxide solution to remove scratches, until the age ring increments on the surface of the sample were clearly observed.

Different parts of the RSS were observed under an Olympus microscope, and images were captured by a charge-coupled device (CCD) at different magnifications (10×, 20×, 40×, 100×, 200×, and 400×). Then, an intact picture was compiled in Photoshop CS 24.0 for the age estimation. The age information of each sample was extracted by two observers. To decrease the bias in age estimation, measurements were considered the effective age when differences in the mean age determined by two observers were less than 10% [30,48]. Given the results of previous studies that compared age estimates collected from cephalopods maintained in artificial feeding conditions and statolith increments with daily beak increments in several species, age and growth patterns can be reliably determined from daily beak increments [20,36,45,46,49]. Additionally, daily beak increments have been successfully used to explore the growth pattern of ommastrephid species in recent years [43,48,51]. Therefore, we explored the growth pattern of *S. oualaniensis* in the South China Sea near the Xisha Islands based on daily beak RSS increments and back calculations of the hatching dates.

## 2.4. Data Analysis

An analysis of covariance (ANCOVA) was used to evaluate whether there were sex differences in ML, BW, and URL growth patterns. We established and selected the optimal growth models to quantify the relationships of ML, BW, and URL with age in *S. oualaniensis*:

Linear function [48,52]:

$$y = a + bt \quad (1)$$

Power function [34,48]:

$$y = at^b \quad (2)$$

Exponential function [48]:

$$y = ae^{bt} \quad (3)$$

Logarithmic function [48]:

$$y = a \ln(t) + b \quad (4)$$

where  $y$  is ML (mm)/BW (g) at age  $t$ ;  $t$  is age (in days); and  $a$  and  $b$  are the parameters to be estimated.

The Akaike information criterion (AIC) was used to compare the 4 types of models. The optimal model was determined and selected based upon the minimum AIC value [35]. The absolute daily growth rate (AGR, mm/d or g/d) and instantaneous growth rate (IGR, %/d) of ML and BW were estimated for each 30-day interval. The AGR and IGR were calculated with the following functions [35,53]:

$$\text{AGR} = \frac{S_2 - S_1}{t_2 - t_1} \quad (5)$$

$$\text{IGR} = \frac{\ln(S_2) - \ln(S_1)}{t_2 - t_1} \quad (6)$$

where  $S_1$  and  $S_2$  represent the mean ML or BW at the beginning  $t_1$  and end  $t_2$  of the time interval, respectively.

All statistical analyses were calculated with RStudio 3.6.0, SPSS 25.0, and Excel 2016; the pictures were processed in Photoshop 2020.

### 3. Results

#### 3.1. Microstructure of the Rostrum Sagittal Section (RSS)

The microstructure characteristics of the RSS of *S. oualaniensis* are shown in Figure 2a. The dark and light bands indicate the daily increments; relatively wide internals are clearly shown on the hood region, and narrower intervals are displayed in the lateral wall region (Figure 2b). It is also easy to identify an inner axis along the boundary between the hood region and lateral wall region, which runs from the rostrum tip to the prong (Figure 2b). Longitudinal increments on the plane of the hood region could be observed more clearly than those on the lateral wall region, which differed in width, patterns, and direction (Figure 2c). The widest internal increments on the RSS were found in the middle region. Each increment in the middle of the inner axis was thicker than the increments at the rostrum tip and prong (Figure 2e). Many distinguishing increments (referred to as the “check” increments) were markedly different from the typical increments (Figure 2e). Additionally, several paler sub-daily increments could be found between the daily increments (Figure 2d). The rostrum tip was often eroded by feeding, preventing the counting of daily increments from the rostrum tip for age estimation (Figure 2e). In terms of the beak pigmentation, the color in the rostrum tip was darker than that in the middle and posterior parts, and the color of the hood region was darker than that of the lateral wall region.

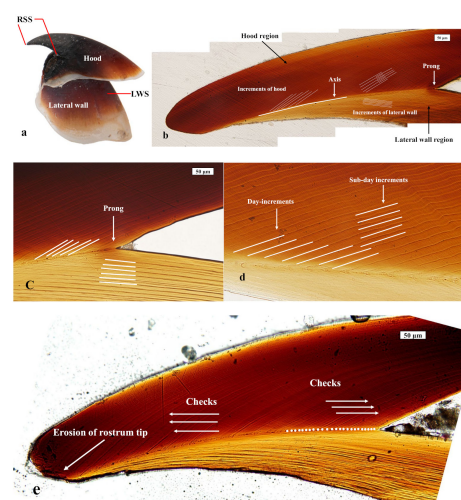


**Figure 2.** The microstructure of the *S. oualaniensis* rostrum sagittal section (RSS). (a) The RSS of the upper beak; (b) microstructure of the RSS; (c) characteristic increments in the hood region and crest region; (d) daily and sub-daily increments; and (e) checks and erosion of the rostrum tip.

### 3.2. Mantle Length and Body Weight

The mantle length (ML) of males ranged from 79 to 153 mm (mean ML:  $112.13 \pm 15.23$  mm), with the majority (80.15%) of samples in the range of 91–130 mm. Female ML ranged from 79 to 200 mm (mean ML:  $119.67 \pm 24.50$  mm), with the majority (76.86%) of samples in the range of 91–130 mm (Figure 3). For maturing and mature squids, the ML of males ranged from 86 to 153 mm and that of females ranged from 115 to 198 mm. The MLs of mature males and females mainly ranged from 70 to 150 mm and from 110 to 210 mm, respectively.

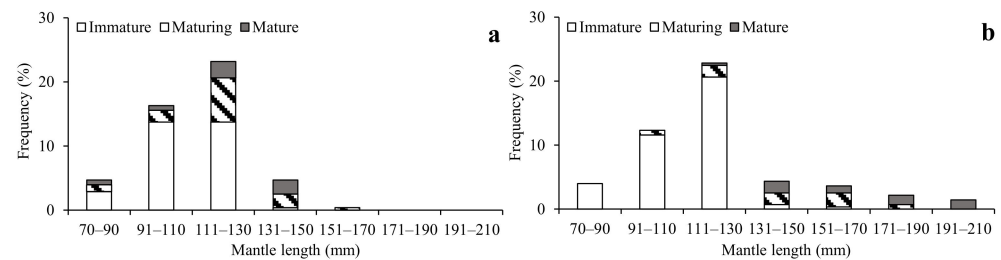


**Figure 3.** Distribution of mantle lengths according to maturity stage for *S. oualaniensis* (a) males and (b) females.

The body weight (BW) of males ranged from 17 to 154 g (mean BW:  $66.97 \pm 29.60$  g), with the majority (85.30%) of samples in the range of 0–100 g. Female BW ranged from 18 to 433 g (mean BW:  $83.59 \pm 68.66$  g), with the majority (82.14%) of samples in the range of 0–100 g (Figure 4).

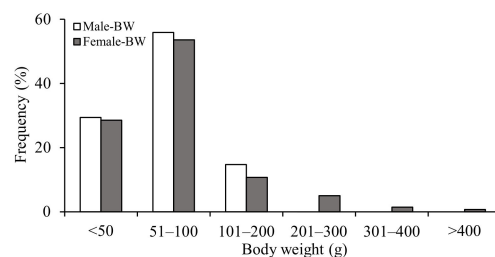


**Figure 4.** Distribution of body weights in both sexes of *S. oualaniensis*.

### 3.3. Age Structure

We successfully estimated the age of 578 beaks (male: 283; female: 295) through examination of daily increments in beak microstructure. Total ages ranged from 97 to 287 days (mean age:  $171.29 \pm 30.18$  days), with the majority (87.32%) of samples in the range of 120–210 days (Figure 5).

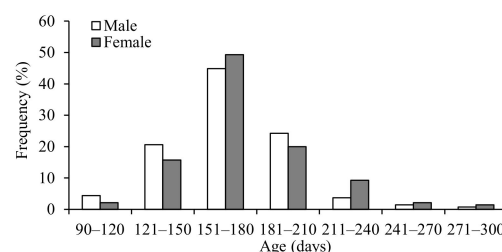


**Figure 5.** Age distribution of *S. oualaniensis* individuals of different sexes.

Male ages ranged from 97 to 287 days (mean age:  $168.37 \pm 29.31$  days), with the majority (88.24%) of samples in the range of 120–210 days. Female ages ranged from 111 to 280 days (mean age:  $174.12 \pm 30.85$  days), with the majority (72.42%) of samples in the range of 150–240 days (Figure 5).

Maturing and mature males were found in every age range, especially at 120–210 days, and maturing and mature females were found at 120–270 days. Females accounted for less than 50% of the total samples (21.35%) (Figure 6).

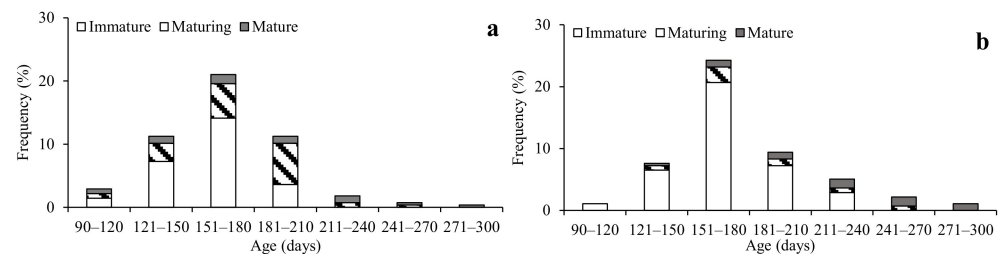


**Figure 6.** Age distribution by maturity stage for *S. oualaniensis* (a) males and (b) females.

### 3.4. Hatching Date and Hatching Group

The back-calculated hatching dates ranged from May to February. The obvious peak hatching period ranged from October to January of the next year (83.33%).

Specifically, the hatching dates of males ranged from May to February, and those of females ranged from June to February. The peak hatching periods for both males and females ranged from October 2017–2019 to January 2018–2020 (males: 80.15%; females: 86.43%). In this study, most samples belonged to the autumn–winter hatching group (Figure 7).

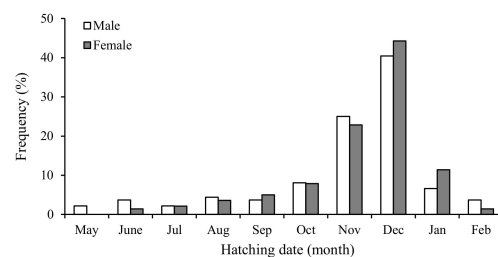


**Figure 7.** Hatching date distribution of *S. oualaniensis* individuals of different sexes.

### 3.5. Growth Patterns

There were significant sex differences in ML ( $f = 0.935$ ,  $p < 0.05$ ) but no sex differences in BW and URL ( $f = 0.145$ ,  $p < 0.05$  and  $f = 1.040$ ,  $p < 0.05$ , respectively).

The age–ML relationships for males and females were both best described by exponential growth models, as they had the lowest Akaike information criterion (AIC) values. The age–BW relationship was best described by the exponential growth model (Figure 8, Table 1), while the age–URL relationship was fitted with the linear growth model (Figure 8, Table 1). The ML–age, BW–age, and URL–age relationships were as follows:

Male ML–age growth model:

$$ML = 70.44e^{0.0029 \times age} (r^2 = 0.5164, n = 283) \quad (7)$$

Female ML–age growth model:

$$ML = 65.27e^{0.0035 \times age} (r^2 = 0.5569, n = 295) \quad (8)$$

BW–age growth model:

$$BW = 16.74e^{0.0084 \times age} (r^2 = 0.5324, n = 578) \quad (9)$$

URL–age growth model:

$$URL = 0.0123 \times age - 265.4640 (r^2 = 0.5124, n = 578) \quad (10)$$

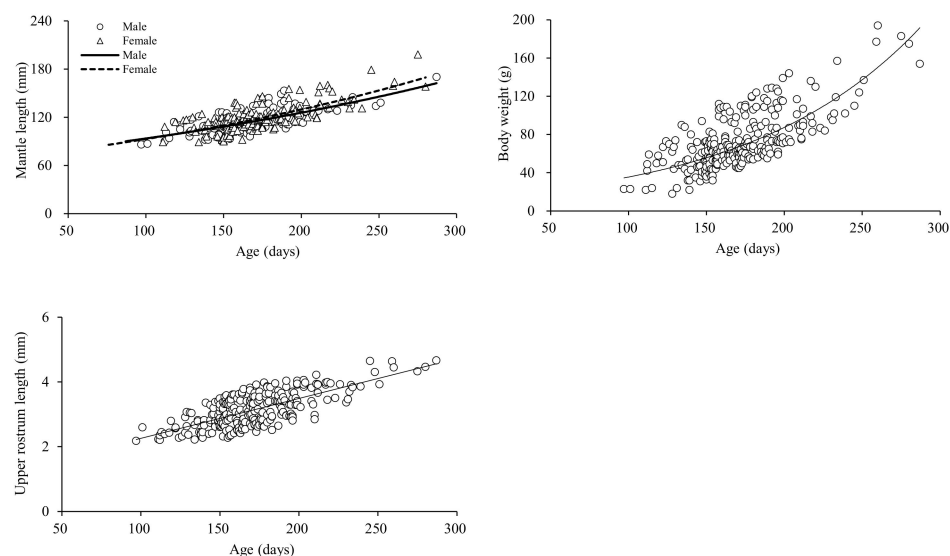


**Figure 8.** The mantle length–age, body weight–age, and upper rostrum length–age relationships in *S. oualaniensis*.

**Table 1.** Parameters of the linear, power, exponential and logarithmic growth models fitted to *S. oualaniensis* mantle length (ML)–age, body weight (BW)–age, and upper rostrum length (URL)–age data.

Growth Model	Linear		Power		Exponential		Logarithmic	
	$r^2$	AIC	$r^2$	AIC	$r^2$	AIC	$r^2$	AIC
Male-ML	0.5154	760.7866	0.3009	810.6165	0.5164	760.5068	0.4990	765.3126
Female-ML	0.5411	844.2501	0.4769	862.5638	0.5569	839.3356	0.5015	855.8462
BW	0.5121	1940.6980	0.3902	2002.2160	0.5324	1928.9760	0.4755	1960.6230
URL	0.5124	−265.4640	0.4693	−250.1230	0.4977	−265.2740	0.4827	−257.1940

### 3.6. Growth Patterns

The growth rate patterns of ML and BW differed between males and females in this study. For males, the maximum absolute daily growth rate (AGR) was 0.36 mm/day for ML during 180–210 days and 0.88 g/day for BW during 240–270 days (Figure 9a). The maximum instantaneous growth rate (IGR) was 0.30 for ML during 120–150 days and 0.90 for BW during 180–210 days (Figure 10a). For females, the maximum AGR was 0.79 mm/day for ML and 1.3 g/day for BW during 240–270 days (Figure 9b). The maximum IGR was 0.50 for ML from 210–240 days and 1.10 for BW from 240–270 days (Figure 10b).

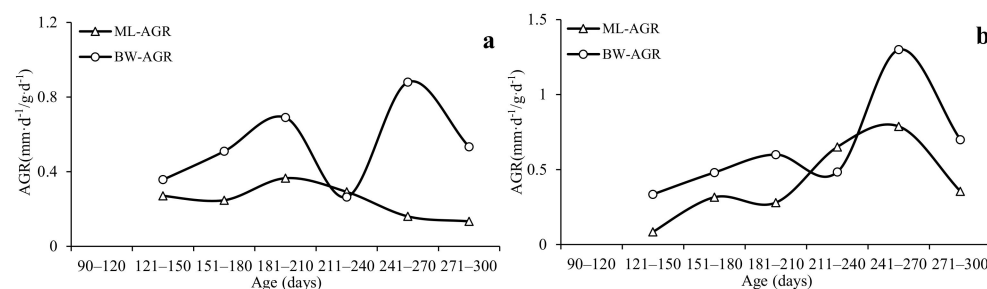


**Figure 9.** Absolute growth rates (AGRs) of mantle length and body weight for *S. oualaniensis* (a) males and (b) females.

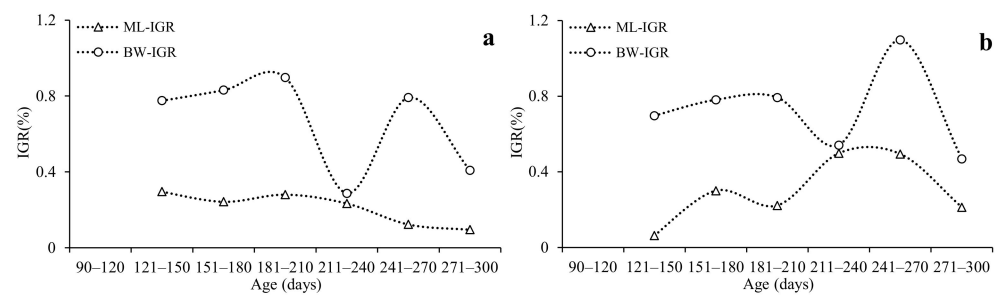


**Figure 10.** Instantaneous growth rates (IGRs) of mantle length and body weight for *S. oualaniensis* (a) males and (b) females.

### 3.7. Age at Maturity

The male-to-female ratio was 1:1.04. A logistic model was used to describe the relationship between the age at the first mature stage in males and females. Males reached the first mature stage more quickly than females for a given size [30]. Specifically, males reached the first mature stage at 128 days, and females reached the first mature stage at 152 days (Figure 11).

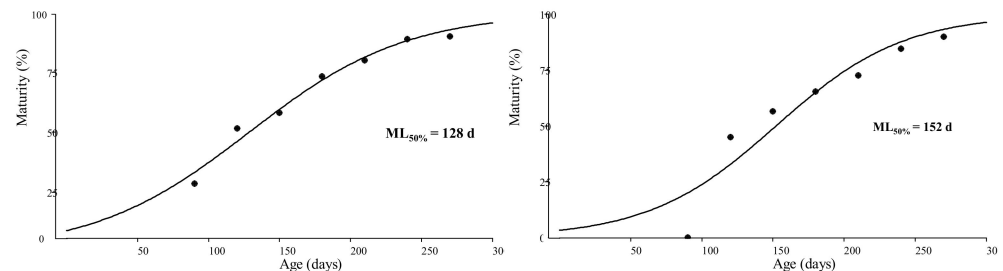


**Figure 11.** Age at first maturity for *S. oualaniensis* males (128 d) and females (152 d).

## 4. Discussion

### 4.1. Beak Microstructure

The usefulness of the beak for determining fishery biology information for cephalopods has been demonstrated; in particular, the upper beak is used to analyze age and growth patterns [36,43,46,48]. In the present study, clear growth increments comprised of light and dark bands were distributed on both sides of the inner axis of the beak; these growth increments exhibited different widths, patterns, and directions on each side. There were significant differences in the direction and width of growth increments between the crest region and lateral wall region. These two increments were joined at the inner axis and regularly displayed in a V pattern. Even though one increment on the lateral wall surface (LWS) can also reflect one day of life history, the rostrum sagittal section (RSS) of the beak is considered to provide a more precise measurement for estimating the age and growth pattern [20,36,45]. Wider intervals between increments in the crest region provide more accurate age estimations than the overlapped narrow intervals in the lateral wall region, although the lateral wall region has lighter pigmentation that allows increments to be more clearly identified [54]. Each increment width in the hood region reflects the growth rate during the early and later stages of life [45]. Narrow increment widths in the rostrum tip and wider increment widths in the middle to the prong could be easily observed in our RSS samples. These patterns demonstrate a faster growth rate in early life history and slower growth in later life history [45].

During feeding, the rostrum tip usually exhibits substantial erosion, which can bias the accuracy of age estimation. However, this problem can be solved by counting the number of increments from the dorsal edge of the hood [45]. Since sub-daily increments may confuse the count, daily increments should be identified carefully to avoid overestimation of the age of *S. oualaniensis*. In this study, obvious checks were displayed in the rostrum tip and prong;

these increments were easily observed and could be distinguished from typical increments. These checks were mostly displayed at early and later stages of life (Figure 2e) and may be evidence of specific events or environmental events that influenced the growth of squids, including periods of environmental change, specific life history stages, and attacks from predators, especially occurring in early and later life [55]. Environmental factors and stress can produce interruptions and delays in beak growth. Thus, the growth pattern of increments was influenced by both external factors and endogenous rhythms [43,56]. Similar increments and checks have also been found in the beak microstructures of other cephalopods and have been applied to studies on the relationships between growth patterns and environmental factors [43,47,48].

#### 4.2. Age Structure and Hatching Group

According to their daily age and capture date, we back-calculated the hatching dates of the *S. oualaniensis* collected in this study. We found that the ages ranged from 97 to 287 days (less than 1 year), which is similar to the typical life span of other ommastrephidae species [35,42,43,48,57]. The majority of males were 120 to 210 days old (life span: 4–7 months), and the majority of females were 150 to 240 days old (life span: 5–8 months) (Figure 6a,b). In this species, males reach maturity more quickly than females of the same age [58], a phenomenon also common in other Ommastrephidae species [59,60]. Previous studies have estimated the life span of *S. oualaniensis* in other areas of the South China Sea with statolith increments; these life spans have mostly been 1–4 months, except for squid collected in the western waters of the Philippines (life span: 95–275 days, 3–9 months) [23,24,26,27,61]. For example, the life span of squid in the Bashi Channel, the eastern tropical Pacific Ocean, the northern Pacific Ocean, and the Bay of Bengal is approximately 2–6 months (53–155 days, 84–168 days, 52–186 days, and 40–120 days, respectively) [22,25,62,63] (Table 2). In addition, squid in the western waters of the Philippines have an estimated life span of 3–9 months (95–275 days) [23]. However, the life span of the giant form of this species that inhabits the northwestern Indian Ocean and Arabian Sea is 4–9 months (120–270 days) [4] and 7 months (203 days), respectively [64] (Table 2). The age structure in our results was approximately half a year, belonging to the dwarf form. This result is also similar to the age structures of forms caught in the Bashi Channel, eastern tropical Pacific Ocean, and western waters of the Philippines [22,23,62,63].

We found that the peak hatching period of males and females occurred from October to January. Therefore, the squid in this study belonged to the autumn–winter hatching group. However, the hatching period of *S. oualaniensis* in the South China Sea in previous studies lasted throughout the year, with peaks from January to March and from July to August (spring/summer/winter hatching groups) [23,26,27,32,61]. Additionally, summer/autumn hatching groups were described in the Bay of Bengal and northern Pacific Ocean from July to October and from May to September [22,25]. Spring and summer hatching groups of *S. oualaniensis* in the northwestern Indian Ocean and Arabian Sea have been recorded, but mixed groups (consisting of four seasons) were also observed along the southwestern coast of India and in Taiwanese waters [4,5,58]. However, the peak hatching periods in the South China Sea, Bashi Channel, eastern tropical Pacific Ocean, and southeastern Arabian Sea were distributed in January, February, and December, representing the winter hatching groups [62,63,65,66] (Table 2).

Body size, food availability, and environmental factors can induce obvious changes in the growth patterns and life spans of squids [67]. Lower temperatures, as in cool high-latitude waters, decrease the growth rate and delay squid maturation. Likewise, higher temperatures, as in warm low-latitude waters, facilitate growth and maturation and reduce life spans [67,68]. Because of the wide distribution and complicated population structures of *S. oualaniensis*, differences in growth patterns and life spans were caused by variation in marine environment factors [1,69]. The spawning season of *S. oualaniensis* has a long duration (1–3 months); after the last spawning, females keep feeding and growing to build up energy for the next spawning [1,70]. There is also evidence that the hatching dates

of *S. oualaniensis* vary. If more mature females are sampled in a given area, this could indicate that the area serves as a spawning ground [71]. According to our results, we suggest that the waters around the Xisha Islands are not the spawning grounds of the autumn–winter hatching group, because mature squid accounted for less than 50% of the total samples [63,71].

**Table 2.** Summary data on *S. oualaniensis* age, peak hatching period and hatching groups in the studied areas.

Study Area	Age (Days)	Peak Hatching Period	Hatching Group	Citation
South China Sea	Medium form: 38–126 Dwarf form: 42–71	Medium form: Jan–Mar Dwarf form: Mar	Winter/spring	[26]
South China Sea	Medium form: 48–125 Dwarf form: 44–95	Medium form: Jul–Aug; Jan Dwarf form: Aug; Jan	Summer/winter	[61]
South China Sea	Medium form: 30–135 Dwarf form: 44–81	Jul–Aug	Summer	[27]
South China Sea	Males: 135–259 Females: 95–275 d	-	Prolonged spawning season	
South China Sea	-	-	Winter	[24]
Bashi Channel	Males: 62–128 Females: 53–155 d	Dec	Winter	
Eastern tropical Pacific Ocean	84–168	Jan–Feb	Winter	[62]
Northern Pacific Ocean	52–186	May–Sep	Summer/autumn	[22]
Bay of Bengal	Males: 40–114 Females: 63–120	Jul–Oct	Summer/autumn	
Northwestern Indian Ocean	120–270	Mar–May	Spring	[4]
Arabian Sea	203	May	Summer	[64]
Southeastern Arabian Sea	-	Dec	Winter	[65]
Southwestern India	-	Medium form: Mar–Apr; Aug–Dec Dwarf form: Feb–Apr; Aug–Nov	Spring/summer/winter	[58]
Taiwanese waters	-	Jun; Sep; Feb–Mar	Spring/summer/autumn/winter	[5]
This study	Males: 121–210 Females: 151–240	Oct–Jan	Autumn/winter	

#### 4.3. Growth Models, Growth Rates, and Maturity

We found a significant sex difference in the relationship between mantle length (ML) and age. From our results, we concluded that the ML–age and body weight (BW)–age relationships were both optimally described by exponential growth models and that the linear growth model best described the upper rostrum length (URL)–age relationship. Previous studies have used various growth models for *S. oualaniensis*. For example, logistic growth models were used to fit the ML–age relationships of both sexes in the Bashi Channel and of males in the South China Sea [61,62]. Linear, power, exponential, and logarithmic growth models were also used to fit the ML–age relationship of other forms in different areas [22,26,61,63]. Similarly, logistic, linear, and power growth models were adopted to describe the BW–age relationship of other forms in different areas [22,61,62]. However, the BW–age relationship was fitted by exponential growth models in our study, similar to the relationships in *D. gigas* and *O. bartramii* [35,40,48]. We also found that the URL increased with increasing daily age, similar to the pattern in *O. bartramii* [48]; increases in size might promote the feeding ability of squids later in life history. This pattern of URL–age demonstrated that the beak grew steadily in this life stage, instead of at a fast rate of growth; therefore, the growth model of URL–age was not fitted into exponential or power growth model which represented rapid growth patterns.

These differences in growth models, especially the ML–age relationship, are obviously affected by variation in environmental factors caused by the wide distribution and

complex population structures of *S. oualaniensis* [67,69]. Previous studies have confirmed that the ML–age growth models of *D. gigas* from different areas show obvious variation as well [35,40]. Based on these studies, we suggest that there is variation in models of *S. oualaniensis* growth depending on the area. Sexual asynchrony in growth rates was reflected in the ML–age relationship and distribution of maturity stages; we found more maturing and mature males and females in early and late life, respectively. Additionally, we found more females with larger sizes (in terms of ML and BW). From the ML–age relationship, it appears that males and females exhibited similar growth rates before 130 days of age, but the ML of females grew more rapidly after 130 days of age. This finding indicates that this age is the inflection point of transformation in the ML growth pattern between males and females. We also suggest that this age may mark the first maturity stage of *S. oualaniensis* in the Xisha Islands waters of the South China Sea. In our study, these models could only be used to analyze the growth relationships during the sub-adult and adult stages; they could not be used for the paralarval and juvenile stages because of the absence of samples.

In our study, all females under 120 days old were immature. From our results, males and females reached the first mature stage at 128 days (4 months) and 152 days (5 months), respectively. The age at first maturity in *S. oualaniensis* from the eastern tropical Pacific Ocean and Bashi Channel (3–4 months) is similar to our results [62,63]. Moreover, similar patterns were found in *D. gigas* [59,72,73], *Illex coindetii* [74,75], and *Illex argentinus* [76]. These results of the first mature stage confirmed that there was sexual asynchrony in the reproduction of males and females. The AGR for male ML was 0.27 mm/day and 0.36 mm/day during 120–150 days and 180–210 days, respectively; the AGR of female ML was 0.32 mm/day and 0.79 mm/day during 150–180 days and 240–270 days, respectively. The AGR of male BW was 0.69 g/day and 0.88 g/day during 180–210 days and 240–270 days, respectively, and that of female ML was 0.60 g/day and 1.30 g/day during 180–210 days and 240–270 days, respectively. The AGR of male ML increased only during 120–210 days and then gradually decreased. The AGR of female ML increased less than males during 120–210 days, but it rapidly increased during 210–270 days. These AGR patterns confirmed the obvious sex differences in the growth of *S. oualaniensis*. Two similar peaks of AGRs of male and female BW were identified: high values during 180–210 days and 240–270 days and low values during 210–240 days. In terms of the life history of *S. oualaniensis*, the paralarval stage is suggested to last approximately 60 days (2 months), followed by the juvenile stage after this stage. Compared to the slower growth rates of the head and body, squid in the paralarval stage exhibit higher growth rates for their arms and fins [65]. Therefore, our finding that the AGRs of ML and BW were lower at 120 days old reflects greater hysteresis in the growth rates of the body compared to those of the arm and fins. Additionally, oceanographic features greatly influence the distribution of cephalopod paralarvae [77]. Because of their poor migratory ability, paralarvae prefer to distribute along the continental shelf edge to feed. Upon the rapid development of their fins, improving their migratory ability, squid can migrate from the continental shelf edge into oceanic waters in the juvenile stage [65]. This transition also marks the improved development for feeding ability of its arms, allowing *S. oualaniensis* to transition among prey items and exhibit cannibalistic behavior in the juvenile stage [65]. After this point, we observed that the AGRs of BW increased greatly during 120–210 days because individuals were able to obtain more food from hunting after changing habitat and prey. In addition, a rapid increase in BW was caused by the development of gonads during 120–210 days. Therefore, we suggested that the paralarval stage finished at approximately 60 days (2 months), followed by the juvenile stage until 120 days of age (4 months). After the juvenile stage, squid enter the sub-adult stage, and this is the age of squid collected in this study.

Males of this species mature faster than females [1]. The reproductive strategy for *S. oualaniensis* females is intermittent multi-batch spawning, and studies have confirmed that these females can spawn continuously during the long spawning season (1–3 months) [1,70].

During the spawning period, the energy is redistributed to primarily provide for the development of gonads instead of body growth, even though the body continues growing at a lower rate, especially detected at maturity stage for tropical species [1,70,78,79]. We observed a gradual decrease in male ML and BW during 180–210 days. Then, BW obviously increased because the development of male gonads was rapid at 210–240 days, but ML continued to exhibit a gradual decrease. These patterns suggest that the growth of male ML gradually stagnated and that the gonads grew continuously during days 210–240. The AGR of ML differed between males and females. Females continue feeding and growing after one spawning behavior. Continuous feeding during 210–240 days of age provides energy for the next spawning [1]; as larger body size is closely correlated with fecundity; females should continue to grow to increase their fecundity [80]. This growth pattern differed from that of males.

## 5. Conclusions

In this study, we have summarized all the results of studies on the age and growth patterns of *S. oualaniensis*. The age and ML ranges in this study indicate that our *S. oualaniensis* samples belong to the autumn/winter hatching group and dwarf form in the South China Sea. We confirmed that the subadult stage occurred at approximately 120–150 days of age (4–5 months). These results suggest that *S. oualaniensis* males and females may first mature at 128 days and 152 days (4–5 months), respectively. After first reproduction, squids grow and feed until the next spawning season (from 210–270 days of age, 7–9 months) in the Xisha Islands waters of the South China Sea. Different age structures, growth patterns, and maturation were caused by its complicated population structure. Our results could provide the basic information for only dwarf form of *S. oualaniensis* in the South China Sea. It is helpful to apply size and age data into assessment management of the dwarf form. However, the growth information could be affected by different sizes and samplings, and also our growth models were not suitably applied to analyze the relationships in early life stage because of the absence of smaller individuals. In the future, we need to expand the sampling area time to obtain, as far as possible, the individuals in the early stage. Meanwhile, exploring and comparing the growth pattern of medium form is also important work for us. These studies would be favorable and helpful for the exploitation and assessment management of resources of *S. oualaniensis* in the South China Sea.

**Author Contributions:** Conceptualization, Z.C. and H.L.; methodology, Z.C., H.L.; software, K.L.; formal analysis, Z.C. and K.L.; investigation, K.L.; resources, H.L. and W.L.; data curation, H.L.; writing—original draft preparation, Z.C.; writing—review and editing, H.L. and X.C.; supervision, H.L. and X.C.; project administration, H.L. and W.L.; funding acquisition, H.L. All authors have read and agreed to the published version of the manuscript.

**Funding:** This research was funded by National Key Research and Development Program of China (2019YFD0901402) and National Natural Science Funding of China (NSFC41506184).

**Institutional Review Board Statement:** The study was conducted according to the guidelines of the Code of Ethics of the University Department of Marine Studies; we only used specimens obtained from the surveys that were already dead.

**Data Availability Statement:** The datasets used and/or analyzed during the current study are available from the corresponding author on reasonable request.

**Acknowledgments:** Support for four scientific surveys made by “QiongSanyaYu 72106” and “QiongSanyaYu 72060” is gratefully acknowledged. We would like to thank to the teachers and students from the laboratory of Shanghai Ocean University for their work and help in sample collection and biological analysis, and for the valuable comments on the revision of the paper.

**Conflicts of Interest:** The authors declare no conflict of interest.

## References

1. Jereb, P.; Roper, C.F.E. *Cephalopods of the World. An Annotated and Illustrated Catalog of Cephalopod Species Known to Date. Volume 2: Myopsid and Oegopsid Squids*; FAO: Rome, Italy, 2010; pp. 315–318.
2. Chesalin, M.V.; Zuyev, G.V. Pelagic cephalopods of the Arabian Sea with an emphasis on *Sthenoteuthis oualaniensis*. *Bull. Mar. Sci.* **2002**, *71*, 209–221.
3. Zuyev, G.V.; Nigmatullin, C.; Chesalin, M.; Nesis, K.N. Main results of long-term worldwide studies on tropical nektonic oceanic squid genus *Sthenoteuthis*: An overview of the Soviet investigations. *Bull. Mar. Sci.* **2002**, *71*, 1019–1060.
4. Chen, X.J.; Liu, B.L.; Tian, S.Q.; Qian, W.G.; Zhao, X.H. Fishery biology of purple-back squid, *Sthenoteuthis oualaniensis*, in the northwest Indian Ocean. *Fish. Res.* **2007**, *83*, 98–104.
5. Okutani, T.; Tung, I.H. Review of biology of commercially important squids in Japanese and adjacent waters. *Symplectoteuthis oualaniensis* (Lesson). *Veliger* **1978**, *21*, 87–95.
6. Zhang, Y. Fisheries Acoustic Studies on the Purpleback Flying Squid Resource in the South China Sea. Master's Thesis, National Taiwan University, Institute of Oceanography, Taipei City, Taiwan, 2005.
7. Zhang, P.; Yang, L.; Zhang, X.F.; Tan, Y.G. The present status and prospect on exploitation of tuna and squid fishery resources in South China Sea. *South China Fish. Sci.* **2010**, *6*, 68–74. (In Chinese with English abstract)
8. Labe, L.L. Catch rate of oceanic squid by jigging method in the South China Sea area III: Western Philippines. In Proceedings of the Third Technical Seminar on Marine Fishery Resources Survey in the South China Sea: Area III, Bangkok, Thailand, 13–15 July 1999; Volume 44, pp. 19–31.
9. Nesis, K.N. Population structure of oceanic ommastrephids, with particular reference to *Sthenoteuthis oualaniensis*: A review. In *Recent Advances in Cephalopod Fishery Biology*; Okutani, T., O'Dor, R.K., Kubodera, T., Eds.; Tokai University Press: Tokyo, Japan, 1993; pp. 375–383.
10. Shchetinnikov, A.S. Feeding spectrum of squid *Sthenoteuthis oualaniensis* (Oegopsida) in the Eastern Pacific. *J. Mar. Biol. Assoc. UK* **1992**, *72*, 849–860. [\[CrossRef\]](#)
11. Parry, M. Feeding behavior of two ommastrephid squids *Ommastrephes bartramii* and *Sthenoteuthis oualaniensis* off Hawaii. *Mar. Ecol. Prog. Ser.* **2006**, *318*, 229–235. [\[CrossRef\]](#)
12. Parry, M. Trophic variation with length in two ommastrephid squids, *Ommastrephes bartramii* and *Sthenoteuthis oualaniensis*. *Mar. Biol.* **2008**, *153*, 249–256. [\[CrossRef\]](#)
13. Markaida, U.; Hochberg, F.G. Cephalopods in the diet of swordfish (*Xiphias gladius*) caught off the West Coast of Baja California, Mexico. *Pac. Sci.* **2005**, *59*, 25–41. [\[CrossRef\]](#)
14. Olson, R.J.; Galván-Magaña, F. Food habits and consumption rates of common dolphinfish (*Coryphaea naiphippurus*) in the Eastern Pacific Ocean. *Fish. Bull.* **2002**, *100*, 279–298.
15. Young, R.E. A brief review of the biology of the oceanic squid, *Symplectoteuthis oualaniensis* (Lesson). *Comp. Biochem. Physiol. Part B Comp. Biochem.* **1975**, *52*, 141–143. [\[CrossRef\]](#)
16. Clarke, M.R. The identification of cephalopod 'beaks' and the relationship between beak size and total body weight. *Bull. Br. Mus. Nat. Hist. Zool.* **1962**, *8*, 419–480.
17. Miserez, A.; Li, Y.; Waite, J.H.; Zok, F. Jumbo squid beaks: Inspiration for design of robust organic composites. *Acta Mater* **2007**, *3*, 139–149.
18. Hernández-García, V. Growth and pigmentation process of the beaks of *Todaropsis eblanae* (Cephalopoda: Ommastrephidae). *Berl. Paläobiologische Abh.* **2003**, *3*, 131–140.
19. Jackson, G.D. The use of beaks as tools for biomass estimation in the deepwater squid *Moroteuthis ingens* (Cephalopoda: Onychoteuthidae) in New Zealand waters. *Polar Biol.* **1995**, *15*, 9–14. [\[CrossRef\]](#)
20. Canali, E.; Ponte, G.; Belcari, P.; Rocha, F.; Fiorito, G. Evaluating age in *Octopus vulgaris*: Estimation, validation and seasonal differences. *Mar. Ecol. Prog. Ser.* **2011**, *441*, 141–149. [\[CrossRef\]](#)
21. Ogden, R.S.; Allcock, A.; Wats, P.; Thorpe, J. The role of beak shape in octopodid taxonomy. *South Afr. J. Mar. Sci.* **1998**, *20*, 29–36. [\[CrossRef\]](#)
22. Takagi, K.; Yatsu, A. Age determination using Statolith microstructure of the purple-back flying squid, *Sthenoteuthis oualaniensis*, in the North Pacific Ocean. *Nippon Suisan Gakkaishi* **1996**, *65*, 98–113. (In Japanese)
23. Zakaria, M.Z.B. Age and growth studies of oceanic squid, *Sthenoteuthis oualaniensis* using statoliths in the South China Sea, Area III, western Philippines. In Proceedings of the SEAFDEC Seminar on Fishery Resources in the South China Sea, Area III: Western Philippines, Bangkok, Thailand, 13–15 July 1999; pp. 118–134.
24. Lu, H.J.; Zhang, X.; Tong, Y.H.; Tang, Y.; Liu, W.; Liu, K.; Chen, X.J. Statolith microstructure and growth characteristics of *Sthenoteuthis oualaniensis* in the Xisha Islands waters of the South China Sea. *J. Fish China* **2020**, *44*, 767–776. (In Chinese with English abstract)
25. Sukramongkol, N.; Promjinda, S.; Prommas, R. Age and reproduction of *Sthenoteuthis oualaniensis* in the Bay of Bengal. In *The Ecosystem-Based Fishery Management in the Bay of Bengal*; Department of Fisheries, Ministry of Agriculture and Cooperatives: Phuket, Thailand, 2007; pp. 195–205.
26. Zhao, C.X.; Chen, Z.P.; He, X.B.; Deng, Y.S.; Feng, B.; Yan, Y.R. Age, growth and population structure of purple back flying squid, *Sthenoteuthis oualaniensis* in the South China Sea in spring based on statolith microstructure. *ACTA Hydrobiol. Sin.* **2017**, *41*, 884–890. (In Chinese with English abstract)

27. Jiang, Y.E.; Chen, Z.Z.; Lin, Z.J.; Qiu, Y.S.; Zhang, P.; Fang, Z.Q. Comparison of fishery biology between medium-form and dwarf-form of *Sthenoteuthis oualaniensis* in South China Sea. *J. Fish China* **2019**, *43*, 454–466. (In Chinese with English abstract)
28. Chen, Z.Y.; Lu, H.J.; Tong, Y.H.; Tang, Y.; Liu, W.; Cheng, X.; Chen, X.J. Beak growth characteristic of *Sthenoteuthis oualaniensis* in the waters of Xisha Island in the South China Sea. *J. Shanghai Ocean Univ.* **2019**, *28*, 373–383. (In Chinese with English abstract)
29. Chen, Z.Y.; Lu, H.J.; Tong, Y.H.; Liu, W.; Zhang, X.; Chen, X.J. Effects of difference of individual size on beak morphology of *Sthenoteuthis oualaniensis* in the Xisha Islands of South China Sea. *J. Fish. China* **2019**, *42*, 2501–2510. (In Chinese with English abstract)
30. Fang, Z.; Xu, L.L.; Chen, X.J.; Liu, B.L.; Li, J.H.; Chen, Y. Beak growth pattern of purpleback flying squid *Sthenoteuthis oualaniensis* in the eastern tropical Pacific equatorial waters. *Fish. Sci.* **2015**, *81*, 443–452. [\[CrossRef\]](#)
31. He, J.R.; Lu, H.J.; Chen, X.Y.; Liu, K.; Wang, H.H.; Chen, X.J. Factors influencing beak morphology of *Sthenoteuthis oualaniensis* in the northwest Indian Ocean. *Chin. J. Appl. Ecol.* **2021**, *35*, 1881–1889. (In Chinese with English abstract)
32. Lu, H.J.; Chen, Z.Y.; Ning, X.; Chen, X.J. Pigmentation change on beak for *Sthenoteuthis oualaniensis* in the Xisha Islands waters of the South China Sea. *Chin. J. Ecol.* **2020**, *39*, 1600–1608. (In Chinese with English abstract)
33. Clarke, M.R. A review of the systematics and ecology of oceanic squids. *Adv. Mar. Biol.* **1966**, *4*, 91–300.
34. Jackson, G.D. Application and future potential of statolith increment analysis in squid and sepiolids. *Can. J. Fish. Aquat. Sci.* **1994**, *51*, 2612–2625. [\[CrossRef\]](#)
35. Chen, X.J.; Lu, H.J.; Liu, B.L.; Chen, Y. Age, growth and population structure of jumbo flying squid, *Dosidicus gigas*, based on statolith microstructure off the Exclusive Economic Zone of Chilean waters. *J. Mar. Biol. Assoc. UK* **2011**, *91*, 229–235. [\[CrossRef\]](#)
36. Hernández-López, J.L.; Castro-Hernández, J.J.; Hernández-García, V. Age determined from the daily deposition of concentric rings on common octopus (*Octopus vulgaris*) beaks. *Fish. Bull.-Natl. Ocean. Atmos. Adm.* **2001**, *99*, 679–684.
37. Agus, B.; Mereu, M.; Cannas, R.; Cau, A.; Coluccia, E.; Follesa, M.C.; Cuccu, D. Age determination of *Loligo vulgaris* and *Loligo forbesii* using eye lens analysis. *Zoomorphology* **2018**, *137*, 63–70.
38. Arkhipkin, A.I.; Shcherbich, Z.N. Thirty years' progress in age determination of squid using statoliths. *J. Mar. Biol. Assoc. UK* **2011**, *92*, 1389–1398. [\[CrossRef\]](#)
39. Hu, G.Y.; Chen, X.J.; Liu, B.L.; Fang, Z. Microstructure of statolith and beak for *Dosidicus gigas* and its determination of growth increments. *J. Fish. China* **2015**, *39*, 361–370. (In Chinese with English abstract)
40. Chen, X.J.; Li, J.H.; Liu, B.L.; Chen, Y.; Li, G.; Fang, Z.; Tian, S.Q. Age, growth and population structure of jumbo flying squid, *Dosidicus gigas*, off the Costa Rica Dome. *J. Mar. Biol. Assoc. UK* **2013**, *93*, 567–573. [\[CrossRef\]](#)
41. Yatsu, A.; Midorikawa, S.; Shimada, T.; Uozumi, Y. Age and growth of the neon flying squid, *Ommastrephes bartramii*, in the North Pacific Ocean. *Fish. Res.* **1997**, *29*, 257–270. [\[CrossRef\]](#)
42. Arkhipkin, A.I.; Mikheev, A. Age and growth of the squid *Sthenoteuthis pteropus* (Oegopsida: Ommastrephidae) from the Central-East Atlantic. *J. Exp. Mar. Biol. Ecol.* **1992**, *163*, 261–276. [\[CrossRef\]](#)
43. Hu, G.Y.; Fang, Z.; Liu, B.L.; Yang, D.; Chen, X.J.; Chen, Y. Age, growth and population structure of jumbo flying squid *Dosidicus gigas* off the Peruvian Exclusive Economic Zone based on beak microstructure. *Fish. Sci.* **2016**, *82*, 597–604. [\[CrossRef\]](#)
44. Moltschanowskyj, N.; Cappel, M. Alternatives to sectioned otoliths: The use of other structures and chemical techniques to estimate age and growth for marine vertebrates and invertebrates. In *Tropical Fish Otoliths: Information for Assessment, Management and Ecology*; Springer: Berlin/Heidelberg, Germany, 2009; pp. 133–173.
45. Perales-Raya, C.P.; Bartolomé, A.; García-Santamaría, M.T.; Pascual-Alayón, P.; Almansa, E. Age estimation obtained from analysis of octopus (*Octopus vulgaris* Cuvier, 1797) beaks: Improvements and comparisons. *Fish. Res.* **2010**, *106*, 171–176. [\[CrossRef\]](#)
46. Perales-Raya, C.P.; Hernández-González, C.L. Growth lines within the beak microstructure of the octopus *Octopus vulgaris* Cuvier, 1797. *S. Afr. J. Mar. Sci.* **1998**, *20*, 135–142. [\[CrossRef\]](#)
47. Perales-Raya, C.P.; Ruzafa, A.J.; Bartolomé, A.; Duque, V.; Carrasco, M.N.; Fraile-Nuez, E. Age of spent *Octopus vulgaris* and stress mark analysis using beaks of wild individuals. *Hydrobiologia* **2014**, *725*, 105–114. [\[CrossRef\]](#)
48. Fang, Z.; Li, J.H.; Thompson, K.; Hu, F.F.; Chen, X.J.; Liu, B.L.; Chen, Y. Age, growth, and population structure of the red flying squid (*Ommastrephes bartramii*) in the North Pacific Ocean, determined from beak microstructure. *Fish. Bull.-Natl. Ocean. Atmos. Adm.* **2016**, *114*, 34–44. [\[CrossRef\]](#)
49. Bárcenas, G.V.; Perales-Raya, C.; Bartolomé, A.; Almansa, E.; Rosas, C. Age validation in *Octopus maya* (Voss and Solís, 1966) by counting increments in the beak rostrum sagittal sections of known age individuals. *Fish. Res.* **2014**, *152*, 93–97. [\[CrossRef\]](#)
50. Lipinski, M.R.; Underhill, L.G. Sexual maturation in squid: Quantum or continuum. *South Afr. J. Mar. Sci.* **1995**, *15*, 207–223. [\[CrossRef\]](#)
51. Liu, B.L.; Chen, X.J.; Chen, Y.; Hu, G.Y. Determination of squid age using upper beak rostrum sections: Technique improvement and comparison with the statolith. *Mar. Biol.* **2015**, *162*, 1685–1693. [\[CrossRef\]](#)
52. Rodhouse, P.G.; Hatfield, E.M.C. Age determination in squid using statolith growth increments. *Fish. Res.* **1990**, *8*, 323–334. [\[CrossRef\]](#)
53. Forsythe, J.W.; Van Heukelem, W.F. *Cephalopod Growth. Cephalopod Life Cycles, Volume II: Comparative Reviews*; Academic Press: London, UK, 1987; pp. 135–155.
54. González, A.F.; Castro, B.G.; Guerra, A. Age and growth of the short-finned squid *Illex coindetii* in Galician waters (NW Spain) based on statolith analysis. *J. Mar. Sci.* **1996**, *53*, 802–810.
55. Arkhipkin, A.I. Statolith as 'black boxes' (life recorders) in squid. *Mar. Freshw. Res.* **2005**, *56*, 573–583. [\[CrossRef\]](#)

56. Kristensen, T.K. Periodical growth rings in cephalopod statoliths. *Dana* **1980**, *1*, 39–51.
57. Quetglas, A.; Morales-Nin, B. Age and growth of the ommastrephid squid *Todarodes sagittatus* from the western Mediterranean Sea. *J. Mar. Biol. Assoc. UK* **2004**, *84*, 421–426. [\[CrossRef\]](#)
58. Chembian, A.J. Studies on the Biology, Morphometrics and Biochemical Composition of the Ommastrephid Squid, *Sthenoteuthis oualaniensis* (Lesson, 1830) of the South West Coast of India. PhD Thesis, Cochin University of Science and Technology, School of Industrial Fisheries, Kochi, India, 2013.
59. Markaida, U.; Quiñónez-Velázquez, C.; Sosa-Nishizaki, O. Age, growth and maturation of jumbo squid *Dosidicus gigas* (Cephalopoda: Ommastrephidae) from the Gulf of California, Mexico. *Fish. Res.* **2004**, *66*, 31–47.
60. Watanabe, H.; Kubodera, T.; Taro, I. Diet and sexual maturation of the neon flying squid *Ommastrephes bartramii* during autumn and spring in the Kuroshio–Oyashio transition region. *J. Mar. Biol. Assoc. UK* **2008**, *88*, 381–389. [\[CrossRef\]](#)
61. Liu, Y.; Wang, X.H.; Du, F.Y.; Liu, B.L.; Zhang, P.; Liu, M.N.; Qiu, Y.S. Age and growth of *Sthenoteuthis oualaniensis* based on statolith microstructure in the South China Sea. *J. Trop. Ocean.* **2019**, *38*, 62–73. (In Chinese with English abstract)
62. Liu, B.L.; Chen, X.J.; Li, J.H.; Chen, Y. Age, growth and maturation of *Sthenoteuthis oualaniensis* in the eastern tropical Pacific Ocean by statolith analysis. *Mar. Freshw. Res.* **2016**, *67*, 1973–1981. [\[CrossRef\]](#)
63. Liu, B.L.; Lin, J.Y.; Feng, C.L.; Li, J.H.; Su, H. Estimation of age, growth and maturation of purple-back flying squid, *Sthenoteuthis oualaniensis*, in Bashi Channel, Central Pacific Ocean. *J. Ocean Univ. China* **2017**, *16*, 525–531. [\[CrossRef\]](#)
64. Sajikumar, K.K.; Najmudeen, T.M.; Ragesh, N.; Jeena, N.S.; Rahuman, S.; Sadanandan-Sunil, K.T.; Sasikumar, G.; Mohamed, K.S. Characterization of an individual of the giant form of the purpleback flying squid *Sthenoteuthis oualaniensis* (Cephalopoda: Ommastrephidae) in the Arabian Sea and its biological descriptors. *Molluscan Res.* **2021**, *41*, 275–284. [\[CrossRef\]](#)
65. Sajikumar, K.K.; Ragesh, N.; Venkatesan, V.; Said-Koya, K.P.; Sasikumar, G.; Kripa, V.; Mohamed, K.S. Morphological development and distribution of paralarvae juveniles of purple back flying squid *Sthenoteuthis oualaniensis* (Ommastrephidae), in the south eastern Arabian Sea. *Vie Milieu Life Environ.* **2018**, *68*, 75–86.
66. Zhao, C.X.; Kang, B.; He, X.B.; Yan, Y.R. Morphological, molecular, and ecological evidence in population determination and fishery management of purpleback flying squid *Sthenoteuthis oualaniensis* in the South China Sea. *Taiwania* **2021**, *66*, 241–250.
67. Arkhipkin, A.I. Diversity in growth and longevity in short-lived animals: Squid of the suborder Oegopsina. *Mar. Freshw. Res.* **2004**, *55*, 341–355. [\[CrossRef\]](#)
68. Mangold, K. Reproduction. In *Cephalopod Life Cycles, Volume II. Comparative Reviews*; Academic Press: London, UK, 1987; pp. 157–200.
69. Keyl, F.; Argüelles, J.; Tafur, R. Interannual variability in size structure, age, and growth of jumbo squid (*Dosidicus gigas*) assessed by modal progression analysis. *ICES J. Mar. Sci.* **2011**, *68*, 507–518. [\[CrossRef\]](#)
70. Harman, R.F.; Young, R.E.; Reid, S.B.; Mangold, K.M.; Suzuki, T.; Hixon, R.F. Evidence for multiple spawning in the tropical oceanic squid *Sthenoteuthis oualaniensis*. *Mar. Biol.* **1989**, *101*, 513–519. [\[CrossRef\]](#)
71. Tafur, R.; Villegas, P.; Rabíand, M.; Yamashiro, C. Dynamics of maturation, seasonality of reproduction and spawning grounds of the jumbo squid *Dosidicus gigas* (Cephalopoda: Ommastrephidae) in Peruvian waters. *Fish. Res.* **2001**, *54*, 33–50. [\[CrossRef\]](#)
72. Mejía-Rebollo, A.; Quiñónez-Velázquez, C.; Salinas-Zavala, C.A.; Markaida, U. Age, growth and maturity of jumbo squid (*Dosidicus gigas* d’orbigny, 1835) off the Western Coast of the baja California peninsula. *Calif. Coop. Ocean. Fish. Investig. Rep.* **2008**, *49*, 256–262.
73. Liu, B.L.; Chen, X.J.; Chen, Y.; Tian, S.Q.; Li, J.H.; Fang, Z.; Yang, M.X. Age, maturation, and population structure of the Humboldt squid *Dosidicus gigas* off the Peruvian Exclusive Economic Zones. *Chin. J. Oceanol. Limnol.* **2013**, *31*, 81–91. [\[CrossRef\]](#)
74. Arkhipkin, A.I.; Jereb, P.; Ragonese, S. Growth and maturation in two successive seasonal groups of the short-finned squid, *Illex coindetii* from the Strait of Sicily (central Mediterranean). *ICES J. Mar. Sci.* **2000**, *57*, 31–41. [\[CrossRef\]](#)
75. Petrić, M.; Škeljo, F.; Šifner, S.K. Age, growth and maturation of *Illex coindetii* (Cephalopoda: Ommastrephidae) in the eastern Adriatic Sea. *Reg. Stud. Mar. Sci.* **2021**, *47*, 101935. [\[CrossRef\]](#)
76. Arkhipkin, A.I.; Laptikhovsky, V. Seasonal and interannual variability in growth and maturation of winter-spawning *Illex argentinus* (Cephalopoda, Ommastrephidae) in the Southwest Atlantic. *Aquat. Living Resour.* **1994**, *7*, 221–232. [\[CrossRef\]](#)
77. Rodhouse, P.G.; Symon, C.; Hatfield, E.M.C. Early life cycle of cephalopods in relation to the major oceanographic features of the southwest Atlantic Ocean. *Mar. Ecol. Prog. Ser.* **1992**, *89*, 183–195. [\[CrossRef\]](#)
78. Arkhipkin, A.I.; Laptikhovsky, V.; Nigmatullin, C.M.; Bespyatykh, A.; Murzov, S.A. Growth, reproduction and feeding of the tropical squid *Ornithoteuthis antillarum* (Cephalopoda, Ommastrephidae) from the central-east Atlantic. *Sci. Mar.* **1998**, *62*, 273–288. [\[CrossRef\]](#)
79. Jackson, G.D. Advances in defining the life histories of myopsid squid. *Mar. Freshw. Res.* **2004**, *55*, 357–365. [\[CrossRef\]](#)
80. Snyder, R. Aspects of the biology of the giant form of *Sthenoteuthis oualaniensis* (Cephalopoda ommastrephidae) from the Arabian Sea. *J. Molluscan Stud.* **1998**, *64*, 21–34. [\[CrossRef\]](#)